

Journal of Applied Remote Sensing

RemoteSensing.SPIEDigitalLibrary.org

Application of a territorial remote radiation monitoring system at the Chernobyl nuclear accident site

Volodymyr Burtniak
Yurii Zabulonov
Maksym Stokolos
Leonid Bulavin
Volodymyr Krasnoholovets

SPIE.

Volodymyr Burtniak, Yurii Zabulonov, Maksym Stokolos, Leonid Bulavin, Volodymyr Krasnoholovets, "Application of a territorial remote radiation monitoring system at the Chernobyl nuclear accident site," *J. Appl. Remote Sens.* **12**(4), 046007 (2018), doi: 10.1117/1.JRS.12.046007.

Application of a territorial remote radiation monitoring system at the Chernobyl nuclear accident site

Volodymyr Burtniak,^a Yurii Zabulonov,^a Maksym Stokolos,^a
Leonid Bulavin,^b and Volodymyr Krasnoholovets^{c,*}

^aInstitute of Environmental Geochemistry under National Academy Science and
Ministry for Emergencies and Affairs of Population Protection from
the Consequences of Chernobyl Catastrophe, Kyiv, Ukraine

^bTaras Shevchenko National University of Kyiv, Physical Faculty, Kyiv, Ukraine

^cInstitute of Physics, National Academy Sciences of Ukraine, Kyiv, Ukraine

Abstract. Dynamic and static characteristics of nonstationary radiation fields are studied. The system on-board of an unmanned aerial vehicle is used for mapping of certain heavily contaminated areas of the Chernobyl nuclear reactor zone. Sources of ionizing radiation under uncertain and unfavorable conditions, with limited time of observation and measurement, have been measured in real time in one single process with a spatial resolution of around 0.5 m and a surface contamination sensitivity of $0.5 \text{ kBq} \cdot \text{m}^{-2}$. Small radioactive spots in an undulating forested area abundantly contaminated with high intensity radioactive isotopes have been plotted on a map. © 2018 Society of Photo-Optical Instrumentation Engineers (SPIE) [DOI: [10.1117/1.JRS.12.046007](https://doi.org/10.1117/1.JRS.12.046007)]

Keywords: aerial monitoring; unmanned aerial vehicle; Chernobyl; radioactive contamination; mapping radiation; nuclear facilities; nuclear waste; remote sensing; digital imaging.

Paper 180381 received May 10, 2018; accepted for publication Sep. 25, 2018; published online Oct. 13, 2018.

1 Introduction

In the third millennium, the world community faces a number of acute challenges. One of the urgent problems is associated with monitoring of nuclear radioactive materials, their containment, and treatment.

Remote sensing of nuclear environmental pollution from an unmanned aircraft is the most effective technology to assess the level of contamination and the dynamics of the spread. Remote radiation monitoring systems allow a quick evaluation of the level of contamination within the physical constraints imposed by a contaminated site.

Aerial remote sensing surveying has a number of advantages over ground-based and space techniques at the detection of radioactive pollution¹⁻³ (see, e.g., Refs. 4-11). In the latter works, the researchers focused on different types of detectors and their construction details, sensitivity of detectors, low altitudes of vehicles (20 to 10 m), their low speed (2 to 4 $\text{m} \cdot \text{s}^{-1}$), and a high spatial resolution (which so far has not exceeded 10 m).

Territorial remote monitoring of the radiation situation under conventional operation of the nuclear power plant in question makes it possible to determine environmental conditions and to identify anomalies and trends in the radiation environment used in the assessment of prospects for further development of nuclear energy. In addition, the territorial remote radiation monitoring of the radiation environment in abnormal and emergency situations is needed to assess the extent of radioactive emissions (discharges) and predict their impact on the surroundings of the nuclear power plant and their service region as a whole (including hydrometeorology and other factors that affect the flow of the propagation of radiation contamination of the environment). This also allows one to refine models of the spread of radioactive contamination identifying the

*Address all correspondence to: Volodymyr Krasnoholovets, E-mail: krasnoh@iop.kiev.ua

effectiveness of measures for decontamination of the contaminated area and the prediction of boundaries of normalization of the radiation environment in time.

To improve the accuracy of understanding of the localization of spatially distributed radioactive sources, new theoretical, methodological, and technical foundations for a space–time analysis of ionization radiation have been developed. This has allowed us to significantly increase the sensitivity of the airborne gamma-system when looking for local sources; in addition, the accuracy and speed of detection of low-level radiative materials and sources of ionizing radiation are also increasing. Our purpose was to find a practical way to do this, with a high degree of sensitivity and accuracy, without having to spend more time than necessary in the contaminated area. So, this work requires a practical approach out of necessity. In this paper, we disclose details of our work on the mapping of areas of the Chernobyl exclusion zone with distributed radioactive spots.

2 Methods

Figure 1 shows a typical setup of radiation sensing and exploration, which we apply to the study of areas contaminated with sources of ionization radiation. In the beginning of the 1990s, we designed and developed an on-board measuring system named the R-Navigator system (it was used on helicopters and later on drones).

In particular, with the help of the R-Navigator system we conducted numerous surveys of the 30-km Chernobyl exclusion zone for radiation mapping of the territory including localization and delineation of areas contaminated with radioactive substances (Fig. 2). Back then, the spatial resolution was quite coarse, around 20 m.

Modern methods allow for a spatial resolution around 10 m. In addition, at high speed and high flight altitude of the airplane some factors need to be considered, such as the volatility (fluctuation) of the natural background radiation and in most cases a low contamination radiation intensity, which both negatively affect the signal-to-noise ratio. Processing such data lead to distortion of the information, and in turn decreases accuracy of the localization and activity measurement of the radioactive source.

These reservations as well as economic factors have led to the need for new measuring radiation monitoring systems embedded in unmanned aerial vehicles (UAVs).

2.1 Measuring System

Zabulonov¹² conducted ground field research analyzing new informative parameters characterizing the dynamic and static characteristics of nonstationary sources of ionization radiation. During 2015 to 2016, we designed an innovative measuring GR-Smart system and developed a new technology of remote radiation monitoring, based on Zabulonov's approach.¹² The remote gamma radiation sensing with an UAV equipped with the "GR-Smart" has been used for mapping of some heavily contaminated areas in the Chernobyl exclusion zone.

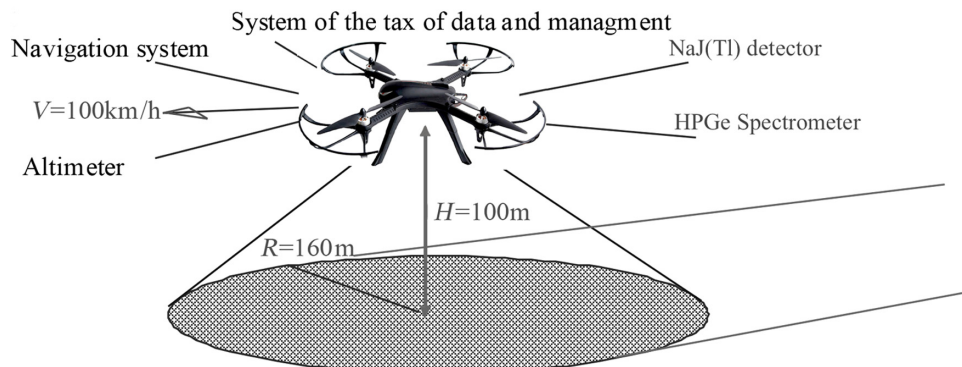


Fig. 1 Remote radiation survey installed in an unmanned aerial vehicle.

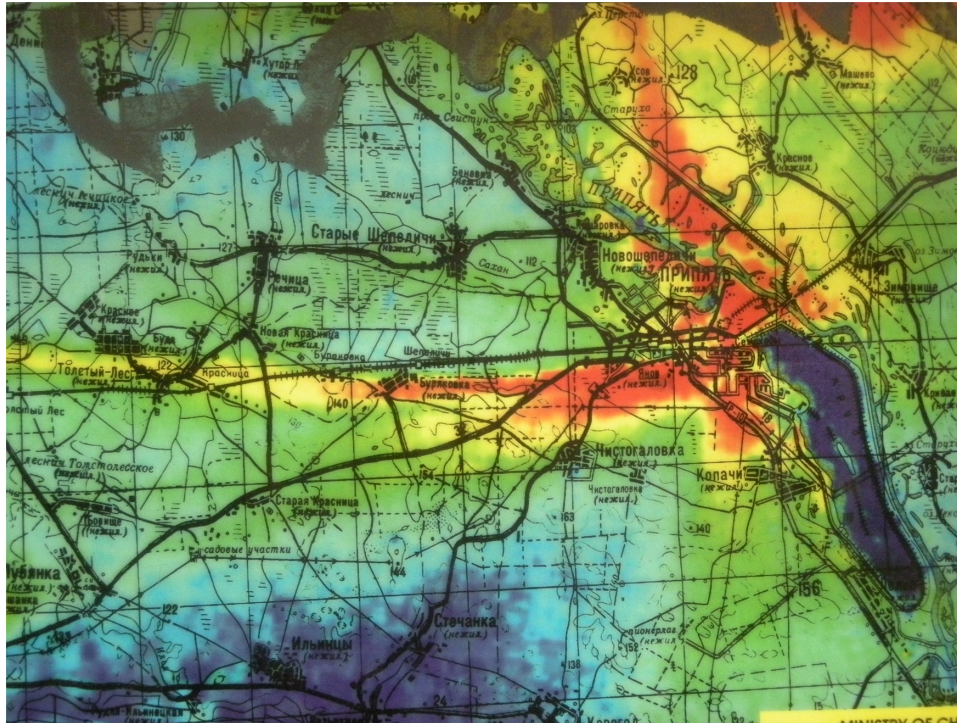


Fig. 2 Radioactive contamination map of the 30-km Chornobyl exclusion zone (with a total area of about 2800 km²) recorded by us with the use of an airplane in 1993. This is the map of the distribution of radiation spots obtained after processing the measurement data obtained from on-board an aircraft. The color indicates the intensity of pollution from “green” (minimum) to “red” (maximum).

The GR-Smart system has enhanced the sensitivity of the system, as well as the probability of detecting nuclear radiation materials and sources of ionizing radiation of low activity in real time, under uncertain and unfavorable conditions, with limited time of observation and measured in a single flight pass. The measurement data are immediately transmitted to the operator on the ground through Wi-Fi.

The areas around the former Chornobyl nuclear power plant are characterized by a high density of surface contamination and contain the entire spectrum of nuclear fuel radionuclides: ¹³⁷Cs, ⁹⁰Sr, ¹⁵⁴Eu, ¹⁵⁵Eu, ²³⁸Pu, ²³⁹Pu, ²⁴⁰Pu, and ²⁴¹Am. Secondary sources of radioactive pollution are also the many points of temporary storage of radioactive waste. Immediately after the accident, two types of temporary radioactive waste storage were introduced: trenches, which are under the ground, and piles, which are above the ground. The size of trenches and piles varies from a few meters up to 10 m in length and width. The height of a pile can be up to 2 m; the trench depth is about 2 m. Currently, trenches and piles are practically inconspicuous because of the subsidence of the soil and thick vegetation cover.

The aim of our study was to create an inventory of the temporal radioactive waste storage locations to determine the need and feasibility of the reburial of the most radioactive waste. The speed of analysis was important to reduce personnel exposure to radioactive sources.

The system for remote monitoring consists of three independent subsystems:

- octocopter-type UAV;
- airborne radiation monitoring subsystem “GR-Smart,” mounted underneath the octocopter;
- ground-based subsystem.

The UAV is used as a carrier for the measuring equipment. The main structural elements of the UAV are:

- control system;
- subsystem for manual management;

- subsystem for automatic control (autopilot);
- gyro stabilised platform that houses the GR-Smart subsystem;
- GPS and other orientation sensors, determining position, velocity, and direction;
- radio channel to communicate with the ground subsystem.

The GR-Smart on-board remote sensing system saves the following parameters during the course of the flight: geographic coordinates, altitude, pressure, temperature, and spectrometric data. The GR-Smart ground system is a computer system that performs:

- processing;
- database maintenance;
- processing of the spectrometric information from the on-board part of the system;
- identification of local zones of radioactive contamination in the measured area;
- determining the spectral composition and the exposure dose of gamma radiation;
- search and determination of coordinates of point sources of gamma radiation;
- construction of a radiation dose outline map image and documentation of the radiation monitoring data;
- transmission of data to the ground via Wi-Fi.

The main element of the measurement system is the spectrometer, an analyzer of gamma radiation based on NaI (TI) scintillation detectors developed by our team. The spectral information is accumulated in the form of an “amplitude-time.” The detection system consists of five NaI detectors. The maximum statistical load of each detector is 2×10^5 pulses \cdot s⁻¹.

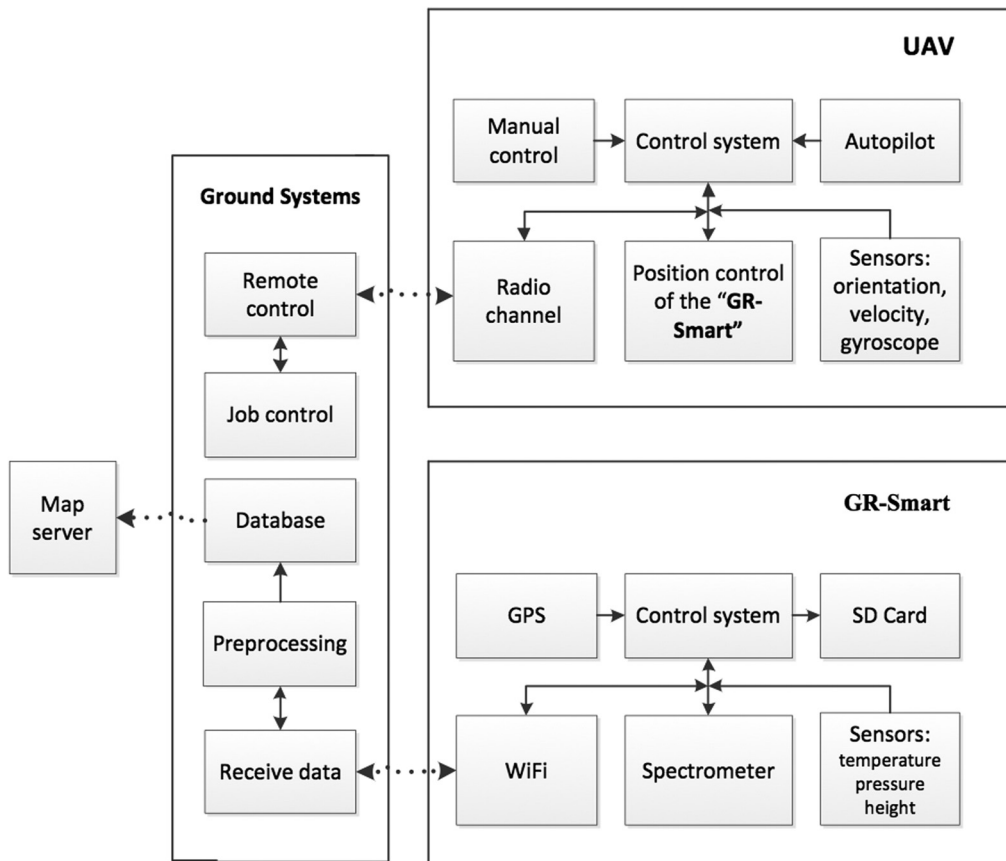


Fig. 3 Block scheme of the system for remote radiation monitoring. Note the radio channel is always active during flight but the Wi-Fi channel is only active when stationary and serves mainly for transmission of stored data. Equipment indicated in the two rightmost boxes is the airborne part of the system. The top connector is real-time data exchange. The bottom connector is batch mode data exchange.

Table 1 Characteristics of the radiation detector mounted on the airplane (1993) and UAV (2016).

Year	1993	2016
Detector	Four NaI(Tl) detectors with diameter 200 mm, height 100 mm	Five NaI(Tl) scintillators with D 63 × 63 (mm)
Sensitivity of dose rate	1.2 $\mu\text{Sv} \cdot \text{h}^{-1}$	0.8 $\mu\text{Sv} \cdot \text{h}^{-1}$
Sensitivity of the density of surface contamination	10 kBq · m ⁻²	0.5 kBq · m ⁻²
Energy range	100 to 3000 keV	30 to 3000 keV
Relative energy resolution for ¹³⁷ Cs	13%	≤6.5%
Exposure time	10 sec	0.1 sec
Speed of the vehicle	45 m · s ⁻¹	2.8 m · s ⁻¹
Height of the flight	200 m	5 to 30 m
Spatial resolution	25 m	0.5 m
Weight	100 kg	10 kg
1-h flight price	\$3000	\$30

Information from all the five detectors is synchronized in one complex “detector.” The Wi-Fi real-time transfer channel transfers signals up to 1000 m.

The major characteristics of the measuring system are shown in Table 1.

The GR-Smart on-board system can inspect 3 km² · h⁻¹. The duration of flight is 40 min. Changing the battery takes 5 min and hence in 1 day the UAV is able to examine 21 km².

The question arises whether the measurements conducted are reliable?

2.2 Calibration

To establish the relationship between the spectrometer readings and the values of the measured radioactive contamination of the terrain, the GR-Smart system was calibrated. For this purpose, a calibration site was prepared; namely, a site of the terrain with previously known certified activity parameters for those radionuclides for which measurements were to be made in the surveyed territories. Measurements of the selected test site with a “manual” spectrometer (one detector Ø 63 × 63 mm); measurements were conducted in the immediate vicinity of the surface (about 0.5 m) by the operator. The results of the measurements are shown in the form of a plan for the distribution of intensities in the terrain (Fig. 4).

Further, we measured the intensities of ionization radiation at a height of 10 m over a part of the test site and a cleaner territory near the study zone. The intensity distribution map is shown in Fig. 5.

Based on the data obtained for the survey of territories, the following arrays of calibration parameters were formed:

- the matrix of linear attenuation coefficients $M = \{R_{ij}\}$. The number of rows of the matrix is equal to the number of radionuclides for which the calibration was carried out, the number of columns is the number of measuring channels of the system. The matrix element R_{ij} is the coefficient of linear attenuation of the total counting rate in the energy window of the radionuclide R_i in the j 'th measuring channel of the system;
- the matrix of normalized contribution coefficients of each measuring channel for each radionuclide $A = a_{ij}$. The dimension of the matrix A is similar to the dimension of the matrix M and is $r \times k$ elements;

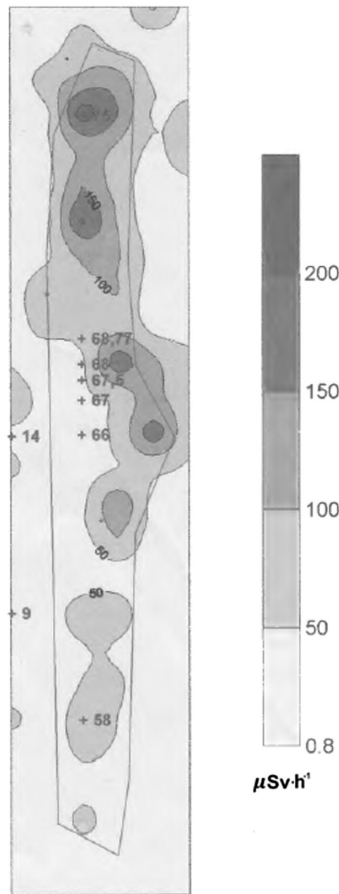


Fig. 4 Calibration area. This is a plot of land in the exclusion zone of the Chernobyl nuclear power plant. Located along the Chernobyl highway, Pripjat.

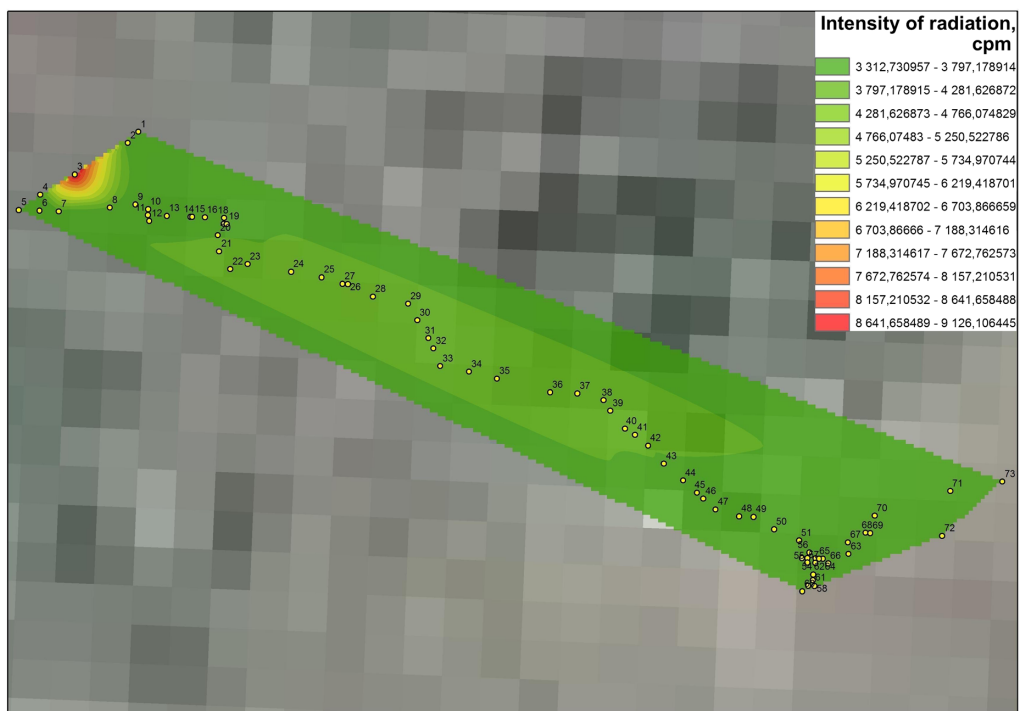


Fig. 5 Flight results of the calibration area.

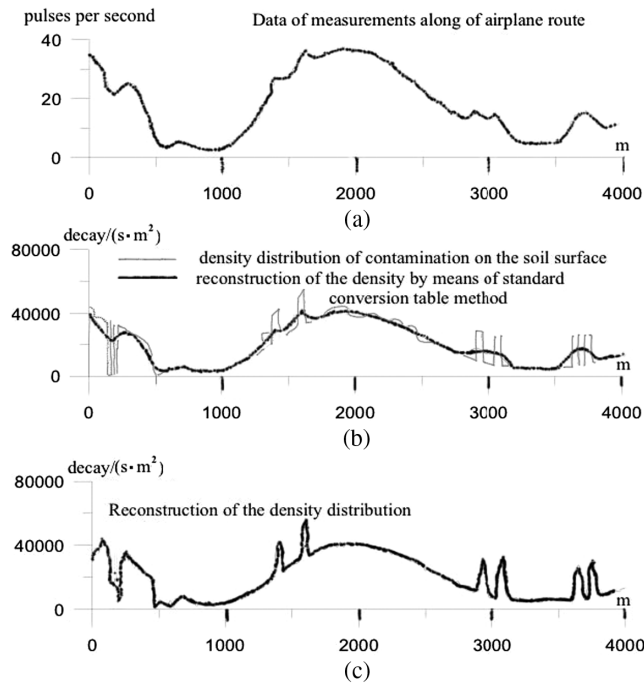


Fig. 6 Parallel testing of both standard conversion table methods for continuous distribution of gamma-sources (time of exposure is 1.0 s; altitude of flight is 70 m; AUV's speed is $28 \text{ m} \cdot \text{s}^{-1}$; aperture is 120 deg). (a) The profile of the detector readings along the flight path; the OY-axis shows pulses per sec, the OX-axis shows meters. (b, c) The source density $\sigma(x, y)$ distributed along the flight path, which is given in decays per second from an area of 1 m^2 . Curve (a) is the data obtained from the sensor along the flight path. The results (curves b and c) are obtained as a result of the solution of the inverse problem at which the density distribution becomes obvious. The curve c is obtained for a standard algorithm (the regularising algorithm) for solving the inverse problem.

- a set consisting of f sensitivity matrices $S_f = S_{ij}(H_f)$ where $S_{ij}(H_f)$ is the sensitivity of the j 'th measuring channel of the system based on the surface activity of the radionuclide R_i when measured from the altitude H_f of the flight LA, where f is the number of modes of measurement for the given height.

Those operations showed a high coincidence of the measurement results (isolated anomalies) with the location of the clamps and trenches (Fig. 6). The existing noncoincidences are mostly explained by the fact that the route of the track passed between the two trenches or the clamps (two objects were influenced by the measurements), as well as the low accuracy of alignment of the obtained images. However, the analysis showed that the low accuracy is mainly caused by additional radioactive stains in the areas under study, which were not marked on the maps.

In the examination discussed, we did not address the issue of identification of radioactive isotopes; it is a separate problem, which was conducted in the framework of our differential method of identification of radionuclides described in a series of works.^{12,13}

The on-board UAV system determined whether there was pollution and revealed radioactive hot-spots. For example, the range of registered activity for ^{137}Cs at the height of 100 m is 0.37 to $3700 \text{ GBq} \cdot \text{km}^{-2}$. The identification of the types of isotopes should be done through a separate dedicated ground station. The data processing methods used in the two different systems (1993 and 2016) are very different: the R-Navigator system collected all the data received on board, whereas the GR-Smart system exchanges the data with the ground in real time.

Examples of the results of the measurements obtained during a flight of the GR-Smart system are shown in Figs. 7 and 8, which show that the UAV has a very high spatial resolution for the separation of point sources and their detection.

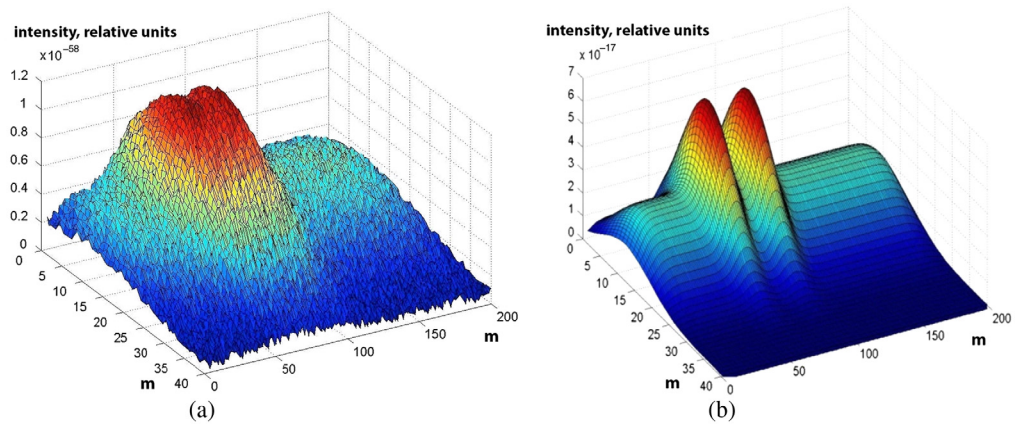


Fig. 7 Spatial resolution of radioactive sources (in different points a and b of the UAV route) of low intensity during the monitoring of local radioactive contaminated areas using the GR-Smart on-board system.

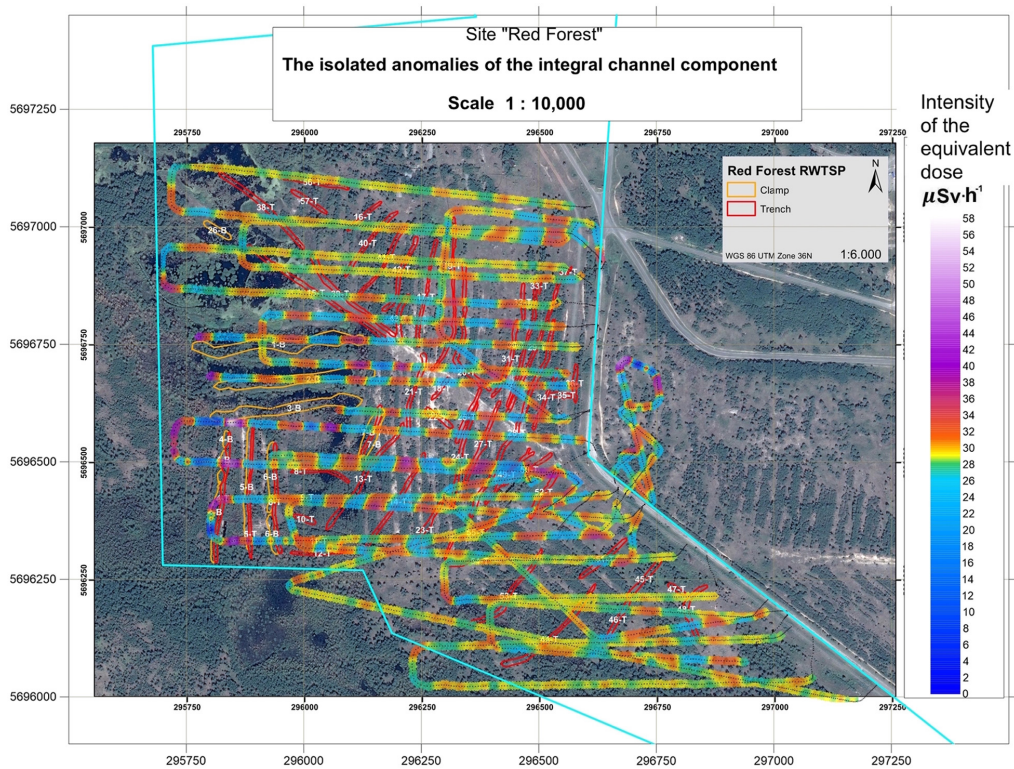


Fig. 8 Overlaying the flight routes on the map of the area. On this map, we mapped radioactive spots along the flight routes. The latter map was obtained using our original processing. By combining them, we can see how our results match with the well-known data recorded after the Chernobyl disaster.

2.3 Inverse Problem Analysis

Solving the inverse problem of the distribution of radioactive contamination on the ground was studied in the previous years; the theory of the phenomenon and the method for solving the reproduction of signals are described in our works.¹⁴⁻¹⁷ In those studies, the mathematical method of exact determination of spatially distributed sources of radiation contamination and renewal of parameters of function of superficial closeness of gamma-radiation was offered.

3 Results and Discussion

Depending on the specific use and technical condition of the system, the number of measuring channels used and the number of altitude measurement modes can be different, i.e., calibration can be performed per channel individually and per specified altitude mode.

To determine the effectiveness of the “aerogamma” survey method, an analysis of the measurements and a comparison of the results obtained with known locations of clamps and trenches on the terrain map are made. For the analysis, representatives of the Chernobyl exclusion zone were provided with only images of maps with graphical marks of clamps and trenches (coordinates were not provided). To determine the effectiveness of the method, the following algorithm has been developed.

For the site under study and for each line, the coordinates of the increased radioactive contamination were determined (Fig. 8). Points in which ionisation radiation was detected above $50 \mu\text{Sv} \cdot \text{s}^{-1}$ were considered as anomalous.

The images of the locations of trenches and clamps obtained by hand were combined with geographic maps and resulted in the coordinates of the investigated terrain.

All geographical coordinates of WGS 84 were transferred to the metric system UTM.

In the vicinity of the coordinates of the points of the selected anomalies, a square with a side of 10 m was highlighted in the image of trenches and clamps.

In this square of the graphic image, red lines were searched (on the resulting images, the boundaries of trenches and clamps are marked in red).

The results of the study are presented in Table 2.

The results of field studies of radioactive contamination in the two most contaminated areas in the Chernobyl exclusion zone carried out in 2015 to 2016 were presented in our papers.^{13,18,19} In those works, we suggested a method of radionuclide measurements that allowed us to distinguish small objects with a high level of ionization radiation and to draw the appropriate maps

Table 2 Results of the survey of the “red forest” site.

Number of track	Spans over trenches	Coincidence (detected radioactive spots match with known trenches and clamps)	Noncoincidences (these detected radioactive spots are additional ones whose locations were previously unknown)
1	7	5	9
2	15	9	7
3	19	10	8
4	20	18	5
5	23	15	3
6	21	19	2
7	26	22	6
8	21	16	5
9	12	12	6
10	8	6	5
11	6	2	7
12	2	1	9
13	5	3	4
14	11	6	2
15	8	7	1

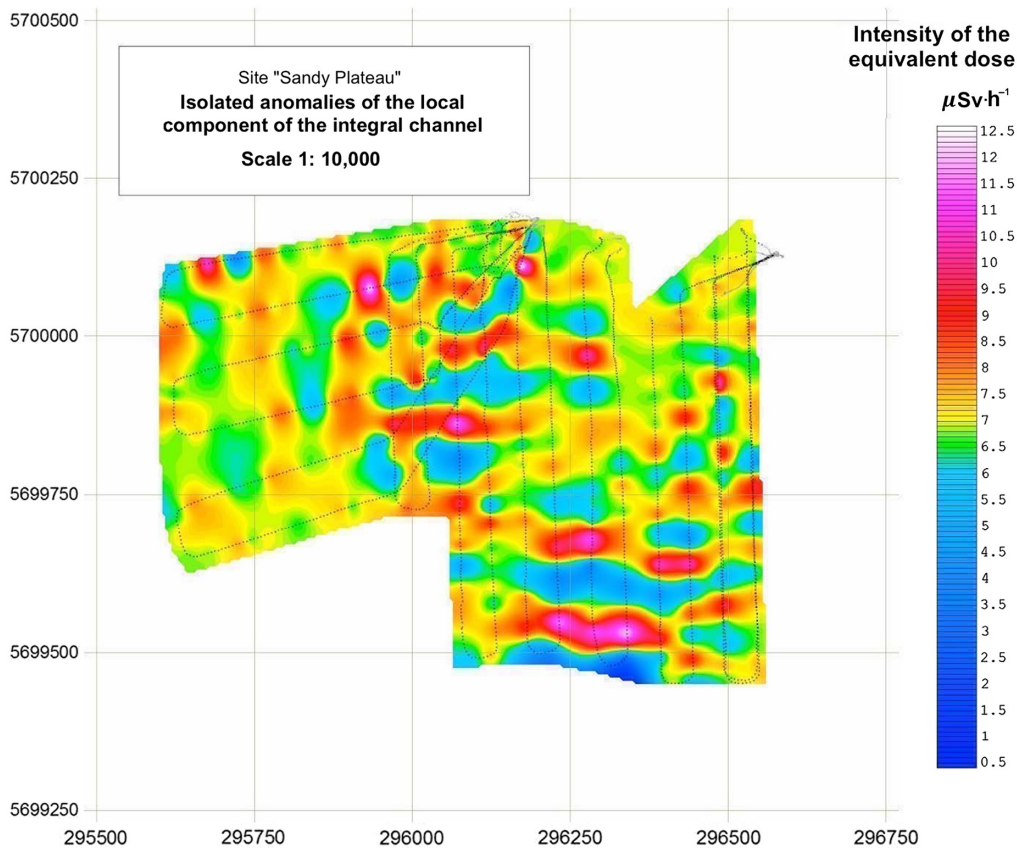


Fig. 9 Components of the distribution of radioactive sources. This figure shows what the distribution of radioactive spots looks like without our original data processing. Data interpolation is performed by ESRI ArcScene software.

of local (high-frequency) components of the observed field with a contour interval equivalent dose of $2 \mu\text{Sv} \cdot \text{h}^{-1}$.

For example, as can be seen from Fig. 9, the eight sections with intensity of 8 to $12 \mu\text{Sv} \cdot \text{h}^{-1}$ are singled out from the general high background of the “Sandy Plateau” site, which in addition were disguised by highly radioactive local trees.

4 Summary

The GR-Smart system allows one to determine radioactive activity in real-time mode. Such timely information on the radionuclides permits one to predict their behavior in the natural environment, which allows monitoring the effectiveness of counter measures to prevent accidents.

The work shows that the GR-Smart system outlined in these studies and used on-board an unmanned aerial vehicle is well suited for localizing and mapping potentially harmful areas with high radiation levels, which has been demonstrated for some areas in the Chernobyl radioactive zone. Our method can work in any type of terrain, even terrain full of pits and hills or densely covered with tall trees. The results that we have obtained are completely in line with our expectations, namely, all the radioactive spots have been clearly detected with a resolution of about 0.5 m.

A number of methods have already been applied to mapping the Fukushima Daiichi radioactive zone. However, they seem to have been unsuccessful as no map of radioactive contaminations has been published yet. We do hope that our method can in the future be used for the Fukushima area, more so because the method allows one to map even sea areas contaminated with radioactive isotopes.

Acknowledgments

The authors thank Alan Cresswell for valuable comments and advice. This work was supported by the NATO Science for Peace and Security (SPS) Programme (Grant No. G5094). We also thank the two anonymous reviewers for their critical reading of the manuscript and the valuable remarks.

References

1. B. Pavlik and J. Engelsmann, "Experience with airborne detection of radioactive pollution (ENMOS, IRIS)," *J. Environ. Radioact.* **72**(1–2), 203–211 (2004).
2. M. J. Kettunen and M. T. Nikkinen, "Fixed-wing gamma measurement for the detection of radioactive materials," *J. Radioanal. Nucl. Chem.* **263**(1), 241–243 (2005).
3. G. Martelet et al., "Classifying airborne radiometry with agglomerative hierarchical clustering: a tool for geologic mapping in context of rainforest (French Guiana)," *Int. J. Appl. Earth Obs. Geoinf.* **8**, 208–223 (2006).
4. S. Okuyama et al., "A remote radiation monitoring system using an autonomous unmanned helicopter for nuclear emergencies," *J. Nucl. Sci. Technol.* **45**(Suppl. 5), 414–416 (2008).
5. R. Pöllänen et al., "Radiation surveillance using an unmanned aerial vehicle," *Appl. Radiat. Isot.* **67**(2), 340–344 (2009).
6. I. Maza et al., "Experimental results in multi-UAV coordination for disaster management and civil security applications," *J. Intell. Rob. Syst.* **61**(1), 563–585 (2011).
7. Y. Sanada et al., "Radiation monitoring using an unmanned helicopter in the evacuation zone around the Fukushima Daiichi nuclear power plant," *Explor. Geophys.* **45**(1), 3–7 (2014).
8. Y. Sanada et al., "The aerial radiation monitoring in Japan after the Fukushima Daiichi nuclear power plant accident," *Prog. Nucl. Sci. Technol.* **4**, 76–80 (2014).
9. S. Chen et al., "Multi-agent patrolling under uncertainty and threats," *PLoS One* **10**(6), e0130154 (2015).
10. D. Connor, P. G. Martin, and T. B. Scott, "Airborne radiation mapping: overview and application of current and future aerial systems," *Int. J. Remote Sens.* **37**(24), 5953–5987 (2016).
11. X.-B. Tang et al., "Efficiency calibration and minimum detectable activity concentration of a real-time UAV airborne sensor system with two gamma spectrometers," *Appl. Radiat. Isot.* **110**, 100–108 (2016).
12. Y. Zabulonov, "The results of modeling and field experiments to identify low-intensity radioactive sources," in *Collection of Scientific Works of the Petukhov Institute of Problems of Modelling in Power*, Vol. 31, pp. 96–100, NAS of Ukraine, Kyiv (2005).
13. Y. Zabulonov, V. Burtnyak, and I. Zolkin, "Airborne gamma spectrometric survey in the Chernobyl exclusion zone based on oktokopter UAV type," *Prob. At. Sci. Technol.* **5**(99), 163–167 (2015).
14. Y. L. Zabulonov, V. V. Kleshchenok, and G. V. Lysyschenko, "Features of detection of local radioactive sources from air vehicles (algorithm, program testing and calculations)," in *Collection of Scientific Works of the G. Petukhov Institute of Problems of Modelling in Power*, Vol. 33, pp. 120–127, NAS of Ukraine, Kyiv (2005).
15. G. V. Lysyschenko et al., "Stochastic regularisation of the inverse problem," in *Collection of Scientific Works of the G. Petukhov Institute of Problems of Modelling in Power*, Vol. 50, pp. 120–127, NAS of Ukraine, Kyiv (2009).
16. Y. L. Zabulonov, G. V. Lisichenko, and G. V. Revunova, "Stochastic regularisation of the inverse problem of reconstructing the radioactivity field parameters from an aero-gamma survey," in *Collection of Scientific Works of the G. Petukhov Institute of Problems of Modelling in Power*, Vol. 52, p. 8, NAS of Ukraine, Kyiv (2009). <http://dspace.nbu.gov.ua/bitstream/handle/123456789/26533/15-Zabulov.PDF?sequence=1>
17. Y. L. Zabulonov, G. V. Lisichenko, and G. V. Revunova, "Improving the efficiency of solving the inverse problem using the projection approach," in *Collection of Scientific Works of the G. Petukhov Institute of Problems of Modelling in Power*, Vol. 53, p. 6, NAS of

Ukraine, Kyiv (2009). <http://dspace.nbu.gov.ua/bitstream/handle/123456789/27082/13-Zabulov.PDF?sequence=1>.

18. Y. L. Zabulonov, V. M. Burtnyak, and L. A. Odukalets, "System for effective remote control and monitoring of radiation situation based on unmanned aerial vehicle," *Sci. Innov.* **13**(4), 40–45 (2017).
19. V. Burtniak et al., "The remote radiation monitoring of highly radioactive sports in the Chernobyl exclusion zone," *J. Intell. Rob. Syst.* **90**(3–4), 437–442 (2018).

Volodymyr Burtniak is an electronic engineer and programmer at the Institute of Geochemistry of Environment, National Academy of Sciences (NAS) of Ukraine. He develops software and designs electronic devices first of all for the measurements of ionize radiation.

Yuri Zabulonov is the correspondent member of NAS of Ukraine. He is the director of the Institute of Geochemistry of Environment, NAS of Ukraine, and the head of the Department of Nuclear Physics Technologies. He has been working in the area of nuclear physics especially studying subtle effects associated with measurements of gamma-, beta-, and alpha-radiation.

Maksin Stokolos is an electronic engineer at the Institute of Geochemistry of Environment, NAS of Ukraine. He develops and designs various electronic devices especially dealing with measurements of electromagnetic-, gamma-, and beta- radiation.

Leonid Bulavin is the academician of NAS of Ukraine. He is the head of the Department of Molecular Physics at the Physics Department of the National Taras Shevchenko University, the head of the Department of Neutron Research Institute of Nuclear Power Plants Safety, and cochair of the Department of targeted training of NAS of Ukraine. He created a scientific school "neutron spectroscopy of condensed matter."

Volodymyr Krasnoholovets is a senior researcher at the Institute of Physics, NAS of Ukraine. His studies cover a wide range of interests including fundamental physics, condensed matter physics, plasma physics, nuclear physics, etc. up to applied sciences.